# SUPPLEMENTARY INFORMATION

# Visualizing Nonlinear Phononics in Layered ReSe$_2$

Junhong Yu,[1] Yadong Han,[1,2] Longyu Wang,[1] Fang Xu,[2] Hang Zhang,[1,2] Yuying Yu,[1] Qiang Wu,[1] Jianbo Hu[1,2,#]

[1]*Laboratory for Shock Wave and Detonation Physics, Institute of Fluid Physics, China Academy of Engineering Physics, Mianyang 621900, China*

[2]*State Key Laboratory for Environment-Friendly Energy Materials, Southwest University of Science and Technology, Mianyang 621010, China*

[#]*To whom correspondence should be addressed. Email: jianbo.hu@caep.cn (JH)*
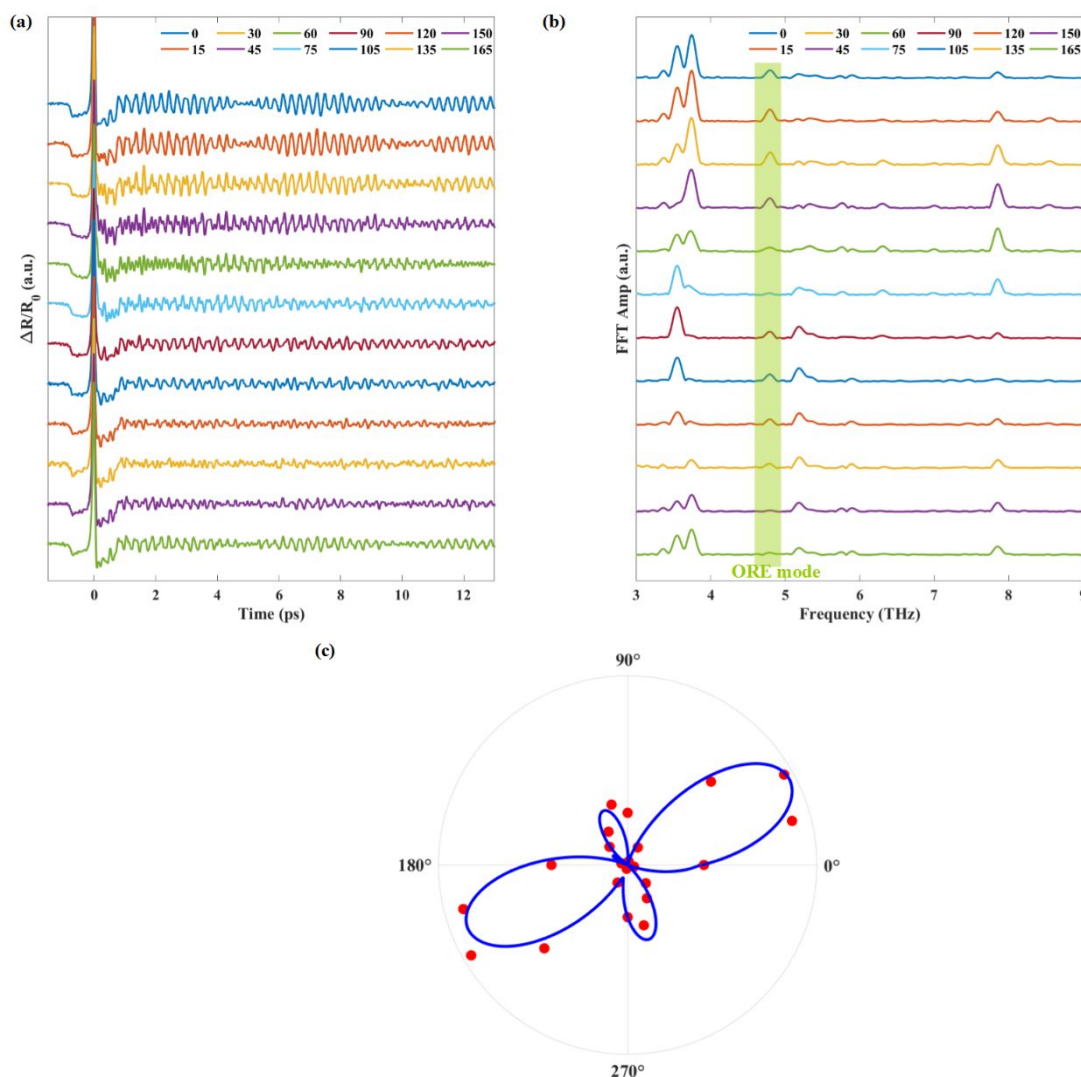
# Supplementary Figure 1



**Figure S1. The direction of Re chains. (a)** Time domain lattice vibrations in layered ReSe2 with different polarization angle of the pump pulse. **(b)** Angular dependence of the corresponding FT spectra. **(c)** Polar plots of the integrated FT amplitude of the ORE mode (4.8-4.9 THz, which is highlighted in Fig. S1b). The solid blue line is a fit to the experimental data.

Following the empirical method proposed by Chenet *et al.*[1] and Lorchat *et al.*[2] for ReX$_2$, the orientation of the Re chains (i.e., the *b*-axis in Fig. 1) in ReX$_2$ has been preliminarily determined by inspecting the angular dependence of the integrated intensity of the ORE mode (the coherent phonon mode at ~4.85 THz, which is denoted as mode V in their works). Based on the polar plot, we can define the reference angle $\theta = \sim 30°$ for a pump pulse polarization parallel to the Re chains.
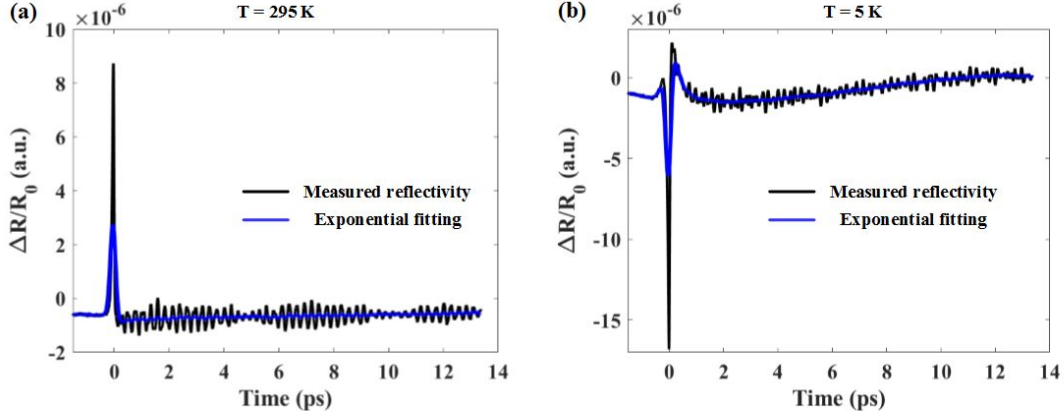
**Supplementary Figure 2**



**Figure S2. Two examples for removing the non-oscillating signal: (a)** T = 295 K and **(b)** T = 5 K.

The reflectivity changes recorded by the balanced PDs are amplified and filtered using the current pre-amplifier and then transferred to the oscilloscope. The oscilloscope averages the voltage wave signal (channel one) over 4000 triggers. Note that these signals need to be divided by the voltage value recorded by one of the balanced PDs and transform the real signal according to the current pre-amplifier. The fast-scan controller produces a signal (channel two) proportional to the pump-probe delay distance, which is recorded by the oscilloscope.

Because the speed of fast-scan is a sine function, the voltage signal after the sine function calibration is used as the time delay of the probe pulse, the data obtained from these two channels of the oscilloscope can well restore the phonon oscillation signal. Spline interpolation was performed on the data for Fourier transform. The band-pass filters of the current pre-amplifier filter most of the non-oscillatory signals, and there are still a small amount of non-oscillating component that need to be processed to remove. Figure S2 shows an example of such data processing, to obtain the pure response of coherent atomic motions in the transient reflectivity, we need to subtract the non-oscillating part (the blue curve) from the measured reflectivity (the black curve).

**Supplementary Table 1**

**Table S1. The comparison of phonon mode frequency measured in Raman spectra and our coherent phonon spectroscopy at room temperature (the ORE mode is highlighted in red)**.

ReSe$_2$ has 12 atoms per unit cell and 36 normal modes are expected. Given the unit cell point group symmetry $C_i$, with only identity and inversion symmetry elements[3], and since all atoms are displaced from the inversion center[4], all normal modes are nondegenerate: there are 18 Raman-active Ag modes, 15 infrared active Au modes, and 3 zero-frequency Au modes. In previous reported Raman study in ReSe$_2$[2,3,5,6], all 18 Raman-active modes have been experimentally observed. Here, in our coherent phonon spectroscopy, up to 13 modes are resolved except those modes with relatively small atomic displacements and short oscillation periods. The good frequency agreement in our experiments with previous Raman study suggests that laser heating effect or photo-induced symmetry transition can be ruled out.

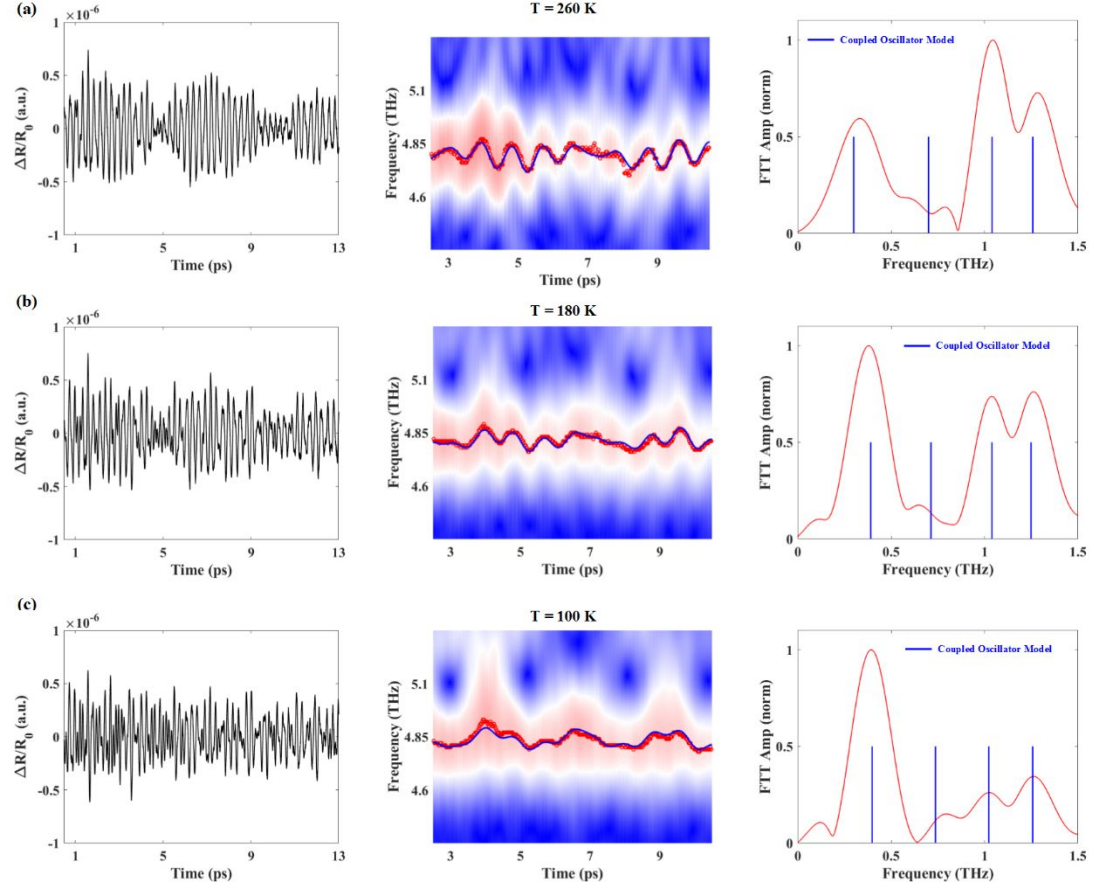| Phonon modes in Raman spectra (cm$^{-1}$)[2-4] | Corresponding frequency of Raman peak (THz) | Phonon modes in our measurements (THz) |
|---|---|---|
| 113.2 | 3.396 | 3.393 |
| 119.7 | 3.591 | 3.581 |
| 125.9 | 3.777 | 3.771 |
| **161.4** | **4.842** | **4.841** |
| 174.4 | 5.232 | 5.244 |
| 179.4 | 5.382 | 5.394 |
| 194.2 | 5.826 | 5.809 |
| 220.6 | 6.618 | 6.563 |
| 234.6 | 7.038 | 7.056 |
| 242.4 | 7.272 | 7.307 |
| 250.4 | 7.512 | 7.533 |
| 263.8 | 7.914 | 7.911 |
| 287.3 | 8.619 | 8.629 |

# Supplementary Figure 3



**Figure S3. Temperature-dependent frequency beating of the ORE mode at 260 K (a), 180 K (b) and 100 K (c).** The pure response of coherent atomic motions in the transient reflectivity ($\Delta R/R_0$) are presented in the left panel. Corresponding SWFT of the ORE mode is shown in the middle panel. Red circles track the peak frequency of the ORE mode at different time delays. The blue solid line is a fitting of the observed frequency beating based on the coupled oscillation model. In the right panel, a FT amplitude spectra (red curves) for the frequency beating of the ORE mode are provided in the right panel. Blue vertical lines are the frequency of coupled LBM frequency extracted from the fitting.
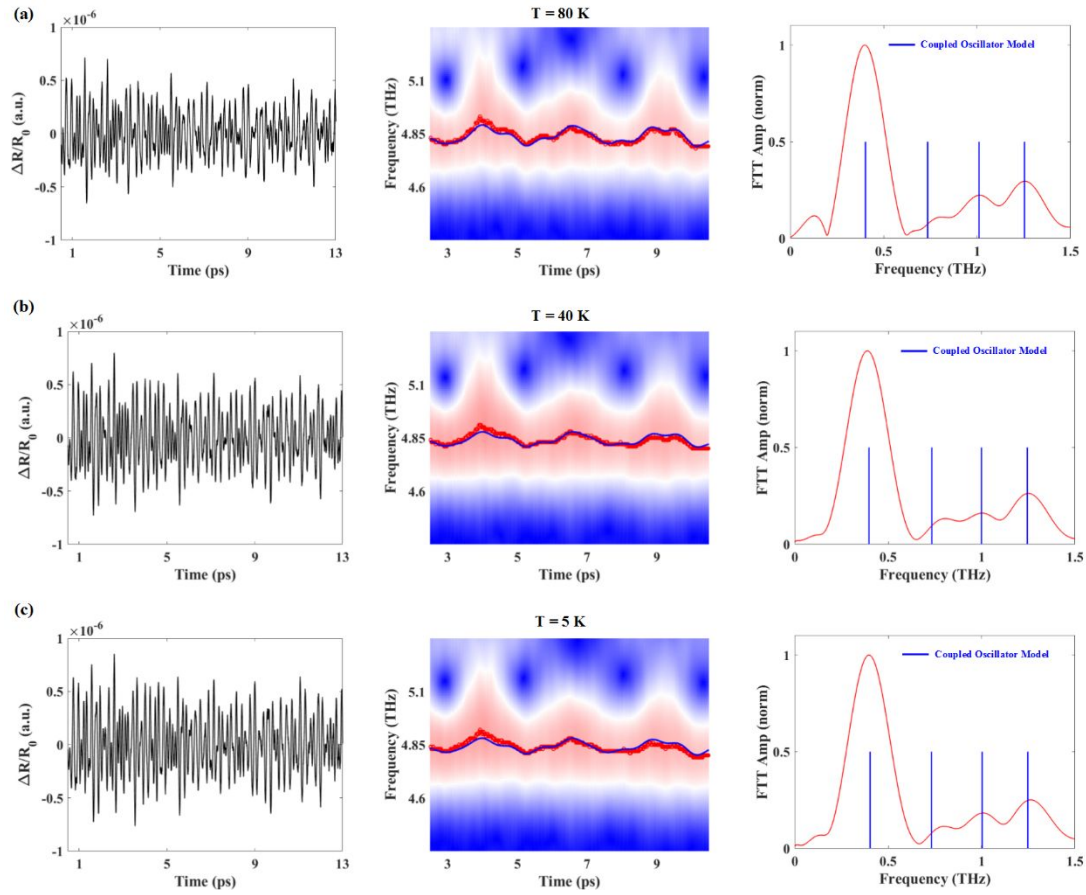
**Supplementary Figure 4**



**Figure S4. Temperature-dependent frequency beating of the ORE mode at 80 K (a), 40 K (b) and 5 K (c).** The pure response of coherent atomic motions in the transient reflectivity ($\Delta R/R_0$) are presented in the left panel. Corresponding SWFT of the ORE mode is shown in the middle panel. Red circles track the peak frequency of the ORE mode at different time delays. The blue solid line is a fitting of the observed frequency beating based on the coupled oscillation model. In the right panel, a FT amplitude spectra (red curves) for the frequency beating of the ORE mode are provided in the right panel. Blue vertical lines are the frequency of coupled LBM frequency extracted from the fitting.

# Reference

1. Chenet, D. A.; Aslan, O. B.; Huang, P. Y.; Fan, C.; van der Zande, A. M.; Heinz, T. F.; Hone, J. C. In-Plane Anisotropy in Monoand Few-Layer $ReS_2$ Probed by Raman Spectroscopy and Scanning Transmission Electron Microscopy. *Nano Lett.* **2015**, 15, 5667-5672.

2. Lorchat, E.; Froehlicher, G.; Berciaud, S. Splitting of interlayer shear modes and photon energy dependent anisotropic Raman response in N-layer $ReSe_2$ and $ReS_2$. *ACS Nano* **2016**, 10, 2752–2760.

3. Wolverson, D.; Crampin, S.; Kazemi, A. S.; Ilie, A.; Bending, S. J. Raman Spectra of Monolayer, Few-Layer, and Bulk $ReSe_2$: An Anisotropic Layered Semiconductor. *ACS Nano* **2014**, 8 (11), 11154–11164.

4. Lamfers, H. J.; Meetsma, A.; Wiegers, G. A.; deBoer, J. L. The Crystal Structure of Some Rhenium and Technetium Dichalcogenides. *J. Alloys Compd.* **1996**, 241, 34–39.

5. Zhao, H.; Wu, J.; Zhong, H.; Guo, Q.; Wang, X.; Xia, F.; Yang, L.; Tan, P.-H.; Wang, H. Interlayer interactions in anisotropic atomically thin rhenium diselenide. *Nano Res.* **2015**, 8, 3651–3661.

6. Kipczak, L.; Grzeszczyk, M.; Olkowska-Pucko, K.; Babiński, A.; Molas, M. R. The optical signature of few-layer $ReSe_2$. *J. Appl. Phys.* **2020**, 128, 044302.